AALBORG UNIVERSITY
STUDENT REPORT

Investigation and Analysis of Thin Diamond Like Carbon Films

3. Semester – Master Project – Autumn 2018

Group 18gr9401

AALBORG UNIVERSITY
STUDENT REPORT

3rd Semester, Master Project

School of Medicine and Health

Biomedical Engineering and Informatics

Frederik Bajers Vej 7A, 9220 Aalborg

Title:
Investigation and Analysis of Thin Diamond Like Carbon Films

Theme:
Applied Biomedical Engineering and Informatics

Project period:
Autumn 2018
01/09/2018 – 20/12/2018

Project group:
18gr9401

Participant:
Annabel Bantle

Supervisors:
Christian Pablo Pennisi
Michael Banghard

Pages:
26

Handed in:
20/12/2018

Synopsis

Improved illuminating systems in operating rooms result in disturbing reflections from conventional surgical instruments. Besides, new labelling requirements for medical devices arise challenges regarding laser markability of surgical instruments.

Diamond like Carbon is an extreme hard dark material with low friction coefficient. Thus Diamond like Carbon is well suited for biomedical applications for example as protective coating with lower reflectivity for surgical instruments.

Laser markability test was conducted in order to investigate, if it is possible to mark Diamond like Carbon with a coherent linear pattern by laser ablation. Surface roughness was measured in order to evaluate, to what extent surface roughness influences Diamond like Carbon coatings and vice versa.

Results of laser markability test showed that it is possible to mark Diamond like Carbon coating with a coherent line pattern by laser ablation. Evaluation of surface roughness measurements showed that the surface roughness of Diamond like Carbon coatings does not hinge on thickness of the Diamond like Carbon coatings, provided that layer defects only occur to a low extent.

Content

1 Introduction

Surgical instruments like scissors, clamps and forceps have to fulfill requirements besides withstanding forces resulting from utilization. Those medical devices are reusable and undergo after each use a cleaning and sterilization cycle. Hence surgical instruments need to be corrosion, wear and scratch resistant. Furthermore biocompatibility and bio-inertness are necessary to prevent chemical and toxic interactions between body tissue and medical device. [1]
In order to reply with these requirements surgical instruments are mainly manufactured from stainless steel and ceramic coatings. [1]

However improved illuminating systems in operating rooms increase disturbing reflections originating from those metallic instruments. Hence instruments with lower reflectivity are necessary. [2] This can be achieved by coating the metallic instruments otherwise than with ceramic coatings and increased instruments' surface roughness [2,3].
Besides this, novel labelling requirements for medical devices result from a new European guideline for medical products. Thus new challenges arise regarding markability of reusable medical devices. [4]

Diamond like Carbon (DLC) is well suited for biomedical applications and is believed to fulfill the requirements. Thin film technology provides opportunities to coat surgical instruments with thin DLC films. [5–7] A method to deposit thin DLC films on substrates is plasma-enhanced chemical vapor deposition (PECVD). This technology is a vacuum based coating process, whereby gas of a chemical compound is used to deposit thin films on a substrate. Plasma provides energy to enhance chemical reactions involved in layer formation. [8–10]

This project was conducted in order to investigate, if it is possible to mark DLC with a coherent linear pattern and to what extent surface roughness influences DLC coatings and vice versa.

2 Background

2.1 Thin Films

The term thin films refers to thin coatings of solid materials. There is no clear definition in the literature describing boundaries for layer thickness of thin films [9,11,12] . However, in practical applications thin films have a thickness in the range of nanometers up to a few micrometers [9,13,14].

Furthermore thin films have physical properties, for example surface roughness and hardness that diverge from the ones of the solid material. Those properties are depending on the coated substrate, film thickness, film surface and deposition method. [9,11] Hence it is possible to achieve properties with thin film technology which would not be available by using the solid material, and thin films can be used to modify surface properties of solids and as protective coatings [13,15–17]. For instance wear and corrosion resistance can be enhanced and friction reduced resulting in extended lifetime of coated items. Moreover hardness, permeation and optical properties like absorption, transmission and reflection can be altered by thin films. [15,16]

Thin films are used in several technical applications like bearings, gears and several tools as well as in electrical, optical or decorative applications like conductors and insulators, glasses, watches and displays. Apart from this thin films are used in medical technology as well. For example as protective coatings on artificial joints or surgical instruments. [16,17] Nonetheless the development of thin film technology is not remaining stationary [13].

2.2 Thin Film Growth

If an atom hits a solid, either it gets reflected or emits energy to the lattice and therefore gets adsorbed. In the latter case it is a so called adatom, which is bounded to the surface but displaceable by lattice vibrations throughout the surface of the solid. Thus adatoms diffuse across the surface of the solid until they desorb or condense. This effect is called random walk. Whilst random walk adatoms emit energy towards the surface of the solid until it condenses or receives energy and condenses. Thereby applies that the energy for desorption equals the energy for adsorption of an adatom. [8]

Throughout film growth applies that celerity of condensation is proportional to temperature on the substrate. In case of low temperature condensation is entailed as soon as two or more adatoms come together on the surface, i.e. fast condensation but layer defects and increased roughness. Whereas high temperature provides the adatoms with more energy. Hence adatoms perform an extended random walk prior to condensation resulting in slow condensation, but low internal stress and lower amount of defects. [8]

Thin film growth can be divided into three mechanisms: [8]

- **Frank-van-der-Merwe growth** occurs if adatoms have more energy and thus extended random walk to arrange themselves in an optimal position. In this case films are deposited layer by layer, i.e. adatoms arrange to replenish the first monolayer before introducing a new layer on top. Frank-van-der-Merwe growth is illustrated in Figure 1a.

- **Vollmer-Weber growth** occurs if adatoms have lower energy and thus condensate as soon as two or more adatoms come together. In this case film growth occurs isle like. Vollmer-Weber growth is illustrated in Figure 1b.
- **Stranski-Krastanov growth** is a hybrid of Frank-van-der-Merwe and Vollmer-Weber growth. Initially complete monolayers as in Frank-van-der-Merwe growth occur, subsequent isle like growth as in Vollmer-Weber growth occurs, resulting in rough films with intergranular porosity. Stranski-Krastanov growth is illustrated in Figure 1c.

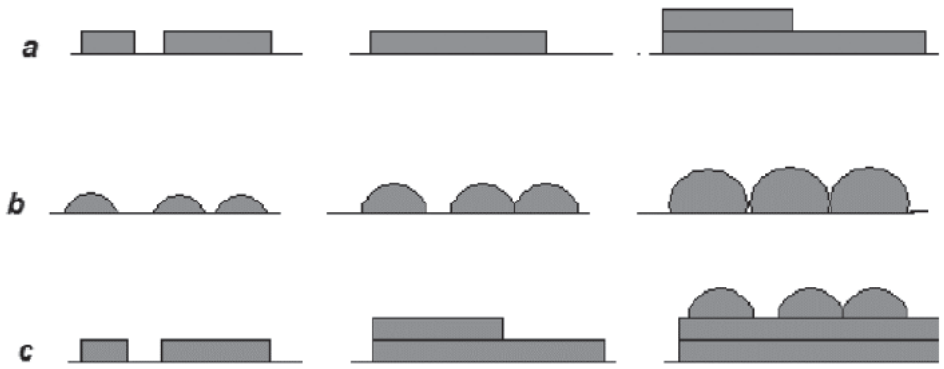

Figure 1: Thin film growth mechanisms. a: Frank-van-der-Merwe growth. b: Vollmer-Weber growth. c: Stranski-Krastanov growth. (Modified [8].)

2.3 Vapor Deposition of Thin Films

Thin films are deposited by vaporizing a target material onto a substrate. There are various deposition techniques which can be mainly divided into two groups, Physical Vapor Deposition (PVD) and Chemical Vapor Deposition (CVD). [8,9]

The main concept of PVD is to vaporize the target material by physical processes like sputtering or evaporation. The vaporized target material is transported to the substrate, where it builds a thin film. The advantages of coatings produced by PVD are, inter alia, good mechanical properties, free from defects and environmental friendliness compared to other coating techniques. [8,9,18]

In CVD reactions of vaporized chemical compounds proceed on the surface of a substrate to deposit a thin film. In order to enhance these reactions energy input is requisite, either in form of heat input or via plasma. [8,9]

Plasma Enhanced Chemical Vapor Deposition (PECVD) is a vacuum based deposition process using plasma as energy input. Plasma consists of electrons, ions and neutral particles. It is generated by an electrical field, which is initiated by a generator. High energy ions and UV radiation of the plasma trigger ionization of reaction gas (precursor) and cause radicals. As a result a film is chemically deposited onto the substrate. Due to prevalent vacuum only a small amount of particles is inside of the process chamber (recipient), thus they can move nearly hitchless. The advantages of PECVD over other CVD processes it that it can be used to coat temperature-sensitive substrates and the adhesion of DLC is enhanced. [8–10]

2.4 Diamond Like Carbon

Carbon occurs naturally in its pure form within two opposite shapes. On the one hand soft and matte graphite and on the other hand hard and shiny diamond. [19]

In graphite are around each carbon atom three carbon atoms arranged on the same level, which can be seen in Figure 2. Hence each atomic layer of graphite's crystal lattice consists of hexagons with sp^2 hybridized atomic bonds. Each atomic layer has a high inner strength, but not in between the layers. Thus the layers can be shifted easily by an external force. This is the reason for the lubricating effect of graphite. [19,20]

In diamond are around each carbon atom four carbon atoms arranged in a tetradic way with sp^3 hybridized atomic bonds, which can be seen in Figure 2. Due to the tetradic structure the binding force between all atoms are very high, resulting in extreme hardness. [19,20]

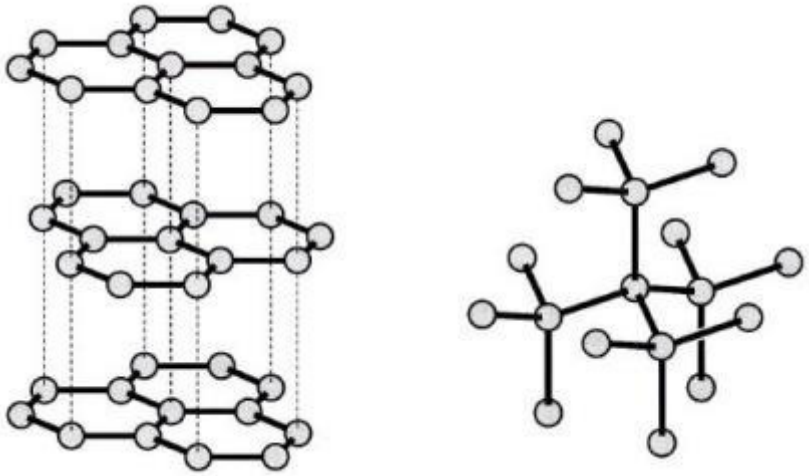

Figure 2: Crystal lattice of graphite (left) and diamond (right). (Modified [20].)

Diamond Like Carbon (DLC) has a mixture of sp^2 hybridized and sp^3 hybridized atomic bonds and thus combines properties of graphite and diamond. DLC films are matte gray to black and possess mechanical properties like extreme hardness, resistance to wear, corrosion and scratches, a low friction coefficient and strong adhesion to various nonmetallic and metallic substrates. Furthermore DLC offers chemical inertness, impermeability and electrical resistivity. Due to its properties DLC is often used as a protective coating for machine tools, automobile components and in military applications. [5–7,21–23]

Apart from this DLC is of great interest for medical applications because of the above mentioned properties and its distinguished biocompatibility. DLC is currently used as coating for artificial joints, medical instruments, heart valves and cardiovascular stents. [5–7]

2.5 Unique Device Identification

The Medical Device Regulation (MDR) from 2017 describes the requirements for conformity assessment of medical devices throughout Europe. MDR stipulates a Unique Device Identification System (UDI-System) for medical devices, which allows tracing of all products and devices. UDI-System is based on international guidelines and principles, which facilitates international reporting of incidents, observation for competent authorities and field safety corrective actions. Potentially UDI-System enables to reduce medical malpractice and counterfeiting. As a result UDI-System enhances efficiency of safety-related actions after products have been placed on the market. Furthermore UDI-System is supposed to enhance procurement policy, inventory control and waste disposal by compatibility with existing authentication systems. [4]

In addition to the UDI-System, an European database for medical devices (Eudamed) is implemented to provide information about medical products and manufacturers. [4]

In order to realize the UDI-System, a Unique Device Identifier (UDI) is required for all medical devices and products, which have been placed on the market, except special products. UDI is a sequence of numerical and alphanumerical signs consisting of a Device Identifier (UDI-DI) and a Production Identifier (UDI-PI). UDI-DI is a unique code assigned to one specific product model and a part of the product's declaration of conformity, whereas UDI-PI provides information about fabrication of a product and may contain lot number, serial number, manufacturing or expiration date. [4]

Since MDR requires that UDI is displayed in human readable form and in machine readable form as linear 1D barcodes, 2D matrix barcodes or radio-frequency identification [4]. An example for UDI labelling is illustrated in Figure 3.

Figure 3: Example of UDI. (Modified [24].)

UDI labelling is an additional requirement and does not replace any other labelling. It is necessary to place UDI on the labels of medical devices and on all packaging levels. Moreover in case of reusable medical devices like surgical instruments, it is required to place UDI directly on the product and not only on the package. [4] Therefore new challenges are set for medical device manufacturer in terms of technical feasibility.

3 Objective

Improved illuminating systems in operating rooms increase disturbing reflections from metallic instruments. Hence it is necessary to develop instruments with lower reflectivity, which can be achieved by coating the metallic instruments and increased surface roughness [2,3]. Since surgical instruments are strongly used and thus undergo many cycles of cleaning and sterilization during their lifetime [1], the coating needs to be wear and scratch-resistant. This can be achieved by dark DLC coatings, which have shown low reflectivity, wear, scratch and corrosion resistance. Besides DLC is biocompatible, which is necessary in order to prevent harms due to toxicity of the coating material. [5–7] Furthermore the MDR requires labelling on these instruments, which is mostly achieved by laser [4]. Therefore the coating needs to be markable by a laser.

Aim of this project was to investigate if it is possible to mark DLC with a coherent linear pattern and to what extent surface roughness influences DLC coatings and vice versa.

This project was conducted in collaboration with the Natural and Medical Sciences Institute (NMI) at the University of Tübingen. The NMI is a business-related research institute focusing on applied research at the interface of life sciences and material sciences. The interdisciplinary research covers the fields of biomedical engineering, surface and material engineering, biotechnology and pharmaceutical engineering. [25]
Concrete the project has been elaborated in the working group Micromedical and Surface Engineering. Remit of Micromedical and Surface Engineering group includes optimizing surfaces of medical devices and manufacturing of flexible electrode systems and implant systems for therapy purposes [25].
Moreover this project was part of the publicly subsidized project LaMaKrO (german: lasermarkierbare Kratzfeste Oberflächen – laser markable scratch resistant surfaces), which aims to develop a matte, dark, laser markable and scratch resistant coating. Project partners processing LaMakrO are, besides NMI, Hochschule Furtwangen University, Ritzi Lackiertechnik GmbH, RUDOLF Medical GmbH + Co. KG and Micromed Medizintechnik GmbH.

4 Methods

4.1 Sample Preparation

Round thin plates (15 mm radius, 2 mm thickness) of stainless steel (Type 1.4301), as illustrated in Figure 4, were used for sample preparation. First the sample number was batched into the back side of in total 170 samples. 135 of the samples were sandblasted, thereof 75 with fine blasting material (grain size 110 µm), 15 with coarse blasting material (grain size 180 to 250 µm) and 45 first with coarse and then with fine blasting material. Pretreatment of samples' surfaces resulted in increased roughness values, which were believed to have an influence to the reflectivity of the coated samples [3]. Samples with and without surface pretreatment are illustrated in Figure 4.

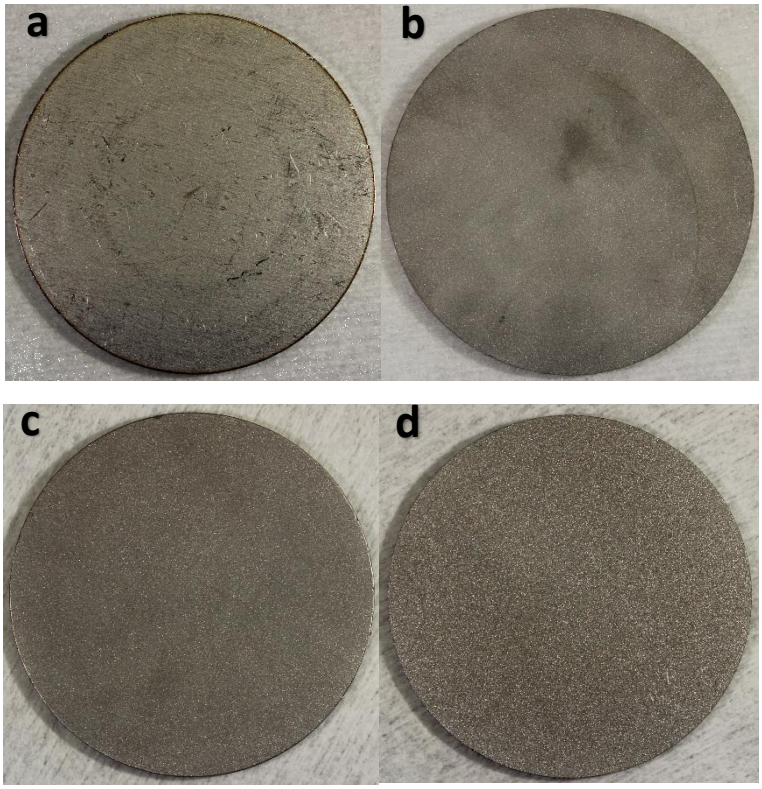

Figure 4a: Sample without surface pretreatment. b: Sample with fine sandblasted surface. c: Sample with coarse and fine sandblasted surface. d: Sample with coarse sandblasted surface.

To remove dust and dirt and inhibit contamination, all samples were cleaned with a washer disinfector DS 50 DRS (Steelco S.p.A.). Following samples were cleaned in an ultrasonic bath for 45 min, thereof 15 min in Acetone and two times 15 min in Isopropanol.

4.2 DLC Deposition

The samples were coated with DLC, because it offers desired properties like wear and scratch-resistance, low reflectivity, a dark surface and biocompatibility [6]. DLC films were deposited by PECVD in thicknesses of 2, 3, 5, 10 and 20 µm. Table 1 shows an overview of pretreatment and coating thickness.

Table 1: Overview of film thickness, pretreatment and amount of coated samples.

Coating thickness	Pretreatment	Number of samples
2 µm	none	5
3 µm	fine sandblasted	20
5 µm	none	5
	fine sandblasted	15
	coarse and fine sandblasted	5
	coarse sandblasted	5
10 µm	none	5
	fine sandblasted	25
	coarse and fine sandblasted	30
	coarse sandblasted	10
20 µm	fine sandblasted	5
	coarse and fine sandblasted	10

The used PECVD system Domino (Plasma Electronic GmbH) is a low pressure system (< 10 Pa), which consists of vacuum pumps, a RF generator to couple energy in, mass flow controller for inserting and regulating precursors and a recipient, which is covered with protective plates. Samples are placed in the recipient on the cathode.

Applied deposition processes consist of various phases. At the beginning the recipient is evacuated by vacuum pumps to reach the start pressure of 0.5 Pa. An Argon plasma is ignited by setting an electric field between recipient's walls and the cathode with the RF generator. Argon plasma pretreatment is used to clean substrate surfaces by ion bombardment. Following by 10 min of Tetramethylsilane (TMS) plasma for enhanced adhesion between DLC and stainless steel. Precursors for DLC deposition are Ethin and TMS in the ratio of 50 sscm : 10 sccm. Thereby working pressure amounts to 1.2 Pa. The deposition rate during a deposition process is 1 µm/h.

Besides the samples, the recipient gets coated during each deposition process. Wherefore the protection plates were sandblasted and recipient as well as protection plates were cleaned with Isopropanol. Following a pre-coating of 150 nm DLC was conducted without samples.

Two different kind of deposition processes were used, either Monolayer or Multilayer deposition process. During the Multilayer deposition process the applied voltage alternates between 400 V and 100 V. As a result of this hard and soft DLC layers are deposited alternating. Thereby one hard and one

soft layer correspond to 1 µm film thickness. Whereas during the Monolayer deposition process the applied voltage remains constant and only hard DLC layers are deposited.

4.3 Raman Spectroscopy

Raman spectroscopy enables to analyze the structural nature of a sample. Therefore a sample is irradiated by a laser, whereby interactions between matter of the sample and the light of the laser occur. Energy is transmitted from light to matter and vice versa. This is called Raman-Effect. This energy transmission results in changes of wavelength (Raman-Shift) which is shown in a Raman spectrum. [26,27]

Raman spectroscopy of DLC provides information about the incidence of sp^2 and sp^3 hybridized atomic bonds in the coating. There are three characteristic peaks for DLC: [26,27]

- **G peak** at approximately 1560 cm^{-1} Raman-Shift is due to oscillating movements, i.e. elongation of hybridized bonds, of each carbon pair with sp^2 hybridized atomic bonds. The intensity of the G peak gives information about the occurrence of sp^2 hybridized atomic bonds and its position gives information about the ratio of sp^3 hybridized atomic bonds.
- **D peak** at approximately 1360 cm^{-1} Raman-Shift is due to breathing modes of sp^2 hybridized lattice sites in rings. The intensity of the D peak gives information about the occurrence of sp^2 hybridized atomic bonds.
- **T peak** at approximately 1060 cm^{-1} Raman-Shift is due to vibrations in sp^3 hybridized atomic bonds. The intensity gives information about the occurrence of sp^3 hybridized atomic bonds. However the T peak can solely be accessed by excitation with a laser in UV wavelength range.

InVia Qontor Raman microscope (Renishaw plc.) was used for Raman spectroscopy. The advantage of inVia Qontor Raman microscope is the possibility to analyze very rough samples. The laser of inVia Qontor has a wavelength of 532 nm. [28] Therewith four samples, which are presented in Table 2, were analyzed by Raman spectroscopy.

Table 2: Overview of samples, which were analyzed by Raman spectroscopy.

Sample	Coating thickness	Process type
067	3 µm	Monolayer process
073	10 µm	Multilayer process
078	3 µm	Multilayer process
087	10 µm	Multilayer process

4.4 Surface Roughness Measurements

A tactile profilometer is a tool to measure surface topography by scanning the surface with a diamond tip. The profilometry delivers 2 or 3D height profiles, whereof several parameters can be determined like the roughness parameters R_a, R_q and R_z: [29–31]

- **Average roughness R_a** is the arithmetic mean of deviation from roughness profile to centerline.
- **Root-mean-squared roughness R_q** is the root mean square of deviation from roughness profile to centerline.
- **Average roughness depth R_z** is determined by the arithmetic mean of deviations from highest to lowest point in each sample length.

The used tactile profilometer is Dektak XT Stylus Profiler (Bruker Corporation). Surface roughness measurements of each sample were conducted before and after DLC deposition. The purpose of surface roughness measurements was to investigate if DLC coatings influence the surface roughness and vice versa. In order to choose an adequate measurement length, a reference piece with predefined roughness was measured over 2, 3 and 4 mm. The best result was achieved by 4 mm measurement length.

Dektak XT Stylus Profiler delivers a height profile of the measured surface [31]. Since the height profile is a combination of form, waviness and roughness of the sample, it is necessary to extract the roughness profile for determination of roughness parameters [29,31]. According to DIN EN ISO 25178 the height profile was filtered by Gaussian regression. [29]
Separating form, waviness and roughness by Gaussian regression filter is seen as minimization problem. Thereby the following function is minimized. [30,32]

$$E(k) = \sum_{l=1}^{n} (z(l) - w(k))^2 \, S(k,l)\Delta x$$

Whereby l is an index for profile points, n the number of points and k an index for position of the weighting function, z denotes the profile element, w the mean line element and Δx the spacing. The weighting function S is defined by the following. Thereby λc denotes the cutoff. [30,32]

$$S(k,l) = \frac{1}{\lambda c \sqrt{\ln(2)}} e^{\left(-\frac{\pi^2}{\ln(2)} \frac{((k-l)\Delta x)^2}{\lambda c^2}\right)}$$

For evaluation of relation between changes in surface roughness pre and post DLC deposition and the film thickness of DLC ANOVA was applied. In order to decide whether One-Way ANOVA or Kruskal-Wallis ANOVA is adequate, Levene's Test was used to evaluate the equality of variances of surface roughness values within film thickness groups. [33]

4.5 Laser Markability

Dumitru et al. [34,35] showed that it is possible to pattern DLC via laser. However it was solely shown that it is possible ablate DLC in form of dots with a diameter of 63±1 µm [34,35]. In order to investigate if it is possible to mark DLC with a coherent linear pattern, the contour of a circle (5 mm diameter) was lasered into DLC coated samples.
ProtoLaser U (LPKF Laser & Electronics AG) was used for laser tests. This pulsed laser is working in UV range with a wavelength of 355 nm. [36]
In total 22 circles were lasered into 6 samples, which can be seen in Figure 5. Circles 1 to 7 were lasered into a 20 µm thick DLC coating, 8 to 13 into a 10 µm, 14 to 18 into a 5 µm and 19 to 22 into a 3 µm thick DLC coating.

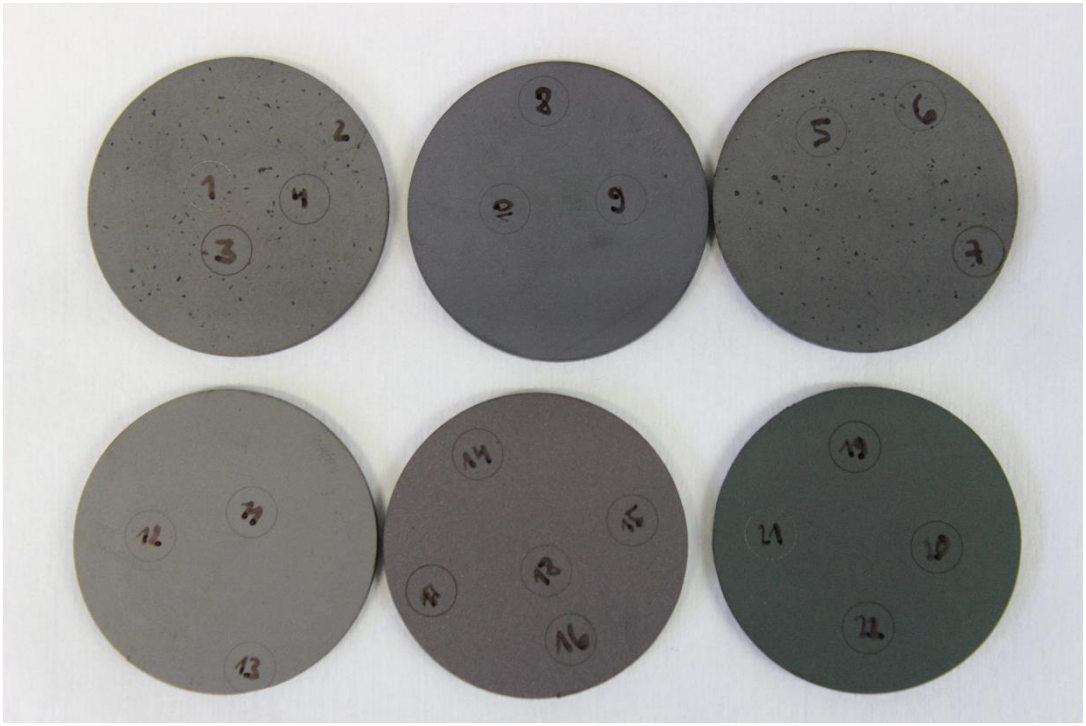

Figure 5: Circles lasered in DLC. Circle 1 to 4 on sample 052, circle 5 to 7 on sample 127, circle 8 to 10 on sample 162, circle 11 to 13 on sample 157, circle 14 to 18 on sample 106 and circle 19 to 22 on sample 077.

In avoidance of destroying the coating and therewith reduce its corrosion and wear resistance, the aim was to ablate enough that a mark remains though little enough that the coating sill protects the surface. Therefore power, frequency, repetitions and mark speed of ProtoLaser U were modified in order to approach adequate settings for those parameters. Table 3 shows the settings of ProtoLaser U for each circle.

Table 3: Overview of ProtoLaser U settings for power, frequency, repetitions and markspeed for each circular laser ablation.

Sample	Circle	Power [W]	Frequency [Hz]	Repetitions	Mark speed $\left[\frac{mm}{s}\right]$
052	1	1	50	10	200
	2	1	50	5	200
	3	1	50	2	200
	4	0.5	50	2	200

Sample	Circle	Power [W]	Frequency [Hz]	Repetitions	Mark speed $\left[\frac{\mathrm{mm}}{\mathrm{s}}\right]$
127	5	0.25	50	2	200
	6	0.25	50	2	250
	7	1.2	40	2	250
162	8	0.25	50	2	250
	9	0.35	75	2	250
	10	0.25	50	2	200
157	11	0.25	50	2	200
	12	0.25	50	2	150
	13	0.25	50	2	100
106	14	0.25	50	2	100
	15	0.25	50	2	200
	16	0.25	50	1	20
	17	0.75	200	1	20
	18	0.75	200	2	200
077	19	0.75	200	1	20
	20	0.75	150	1	20
	21	0.75	50	2	20
	22	0.25	50	2	200

Thereafter the samples have been cleaned in an ultrasonic bath for 15 min with Isopropanol. This ensured that all particles, remaining after laser ablation, are removed. For evaluation if it was ablated enough that a mark remains without uncovering stainless steel underneath, each circle has been inspected with a light microscope with 50 fold magnification.

5 Results

5.1 Sample Preparation

DLC coating flaked off samples without pretreatment, whereas flaking did not occur on sandblasted samples. No difference in flaking was observed between fine, coarse and fine or coarse sandblasted samples. Figure 6 illustrates from left to right samples without pretreatment, fine sandblasted, coarse and fine sandblasted and coarse sandblasted samples. Thereby the top row was coated by using 10 µm Multilayer processes and the bottom row was coated by using 5 µm Multilayer processes.

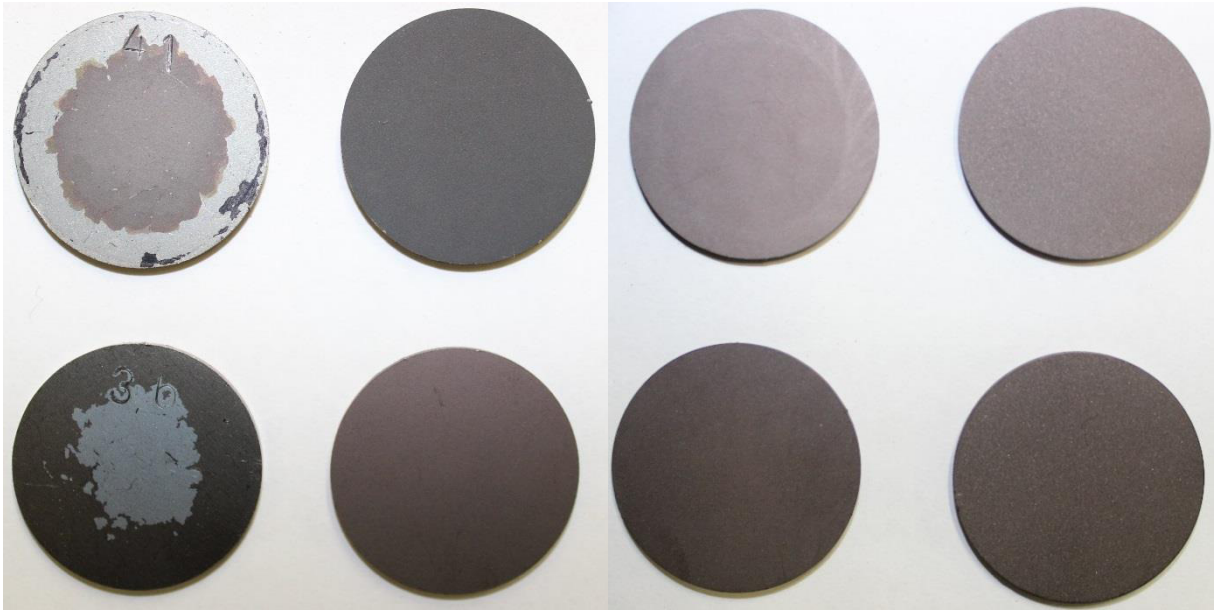

Figure 6: From left to right DLC coated samples without pretreatment, fine sandblasted, coarse and fine sandblasted, and coarse sandblasted. Thereby the upper row coated with 10 µm and the lower row with 5 µm Multilayer DLC.

5.2 DLC Deposition

Deposition processes resulted in different colored DLC coatings. Although the same processes were applied on different days or with varied coating thickness, the color of deposited DLC differs. Examples are shown in Figure 7. For instance a 3 µm Monolayer process resulted in a brownish coating (Figure 7 a), a 10 µm Multilayer process resulted in dark grey coating (Figure 7 b), a 3 µm Multilayer process resulted in a greenish coating (Figure 7 c) and another 10 µm process resulted in light grey coating (Figure 7 d).

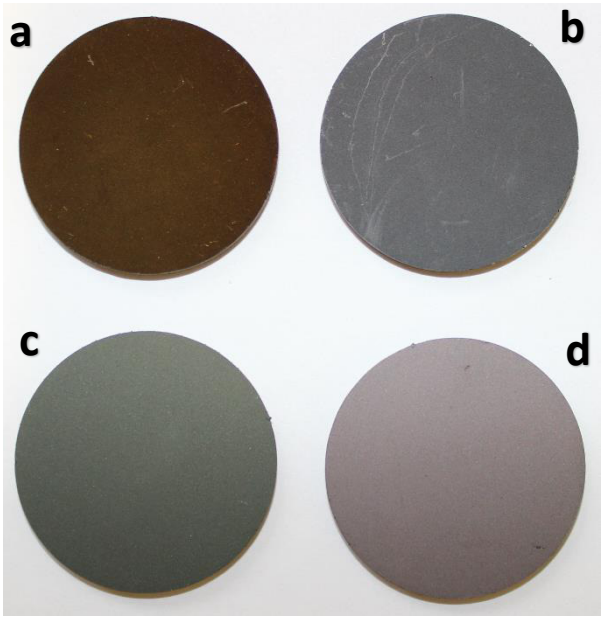

Figure 7: DLC coated samples with different colors. a: Sample 067 coated with 3 µm Monolayer process. b: Sample 073 coated with 10 µm Multilayer process. c: Sample 078 coated with 3 µm Multilayer process. d: Sample 087 coated with 10 µm Multilayer process.

5.2 Raman Spectroscopy

The Raman spectrum, illustrated in Figure 8, shows for all samples the D peak at approximately 1360 cm^{-1} Raman Shift and the G peak at approximately 1560 cm^{-1} Raman Shift. However D and G peak position is not the same for all samples and varies for D peak between 1320 and 1360 cm^{-1} Raman Shift, and for G peak between 1570 and 1590 cm^{-1} Raman Shift. D and G peak are for samples 067, 073 and 078 well separated, whereas for sample 087 D and G peaks are overlapping due to different peak widths of the samples. Furthermore the intensity of D and G peak is highest in samples 078 and 087, and lowest in sample 067.

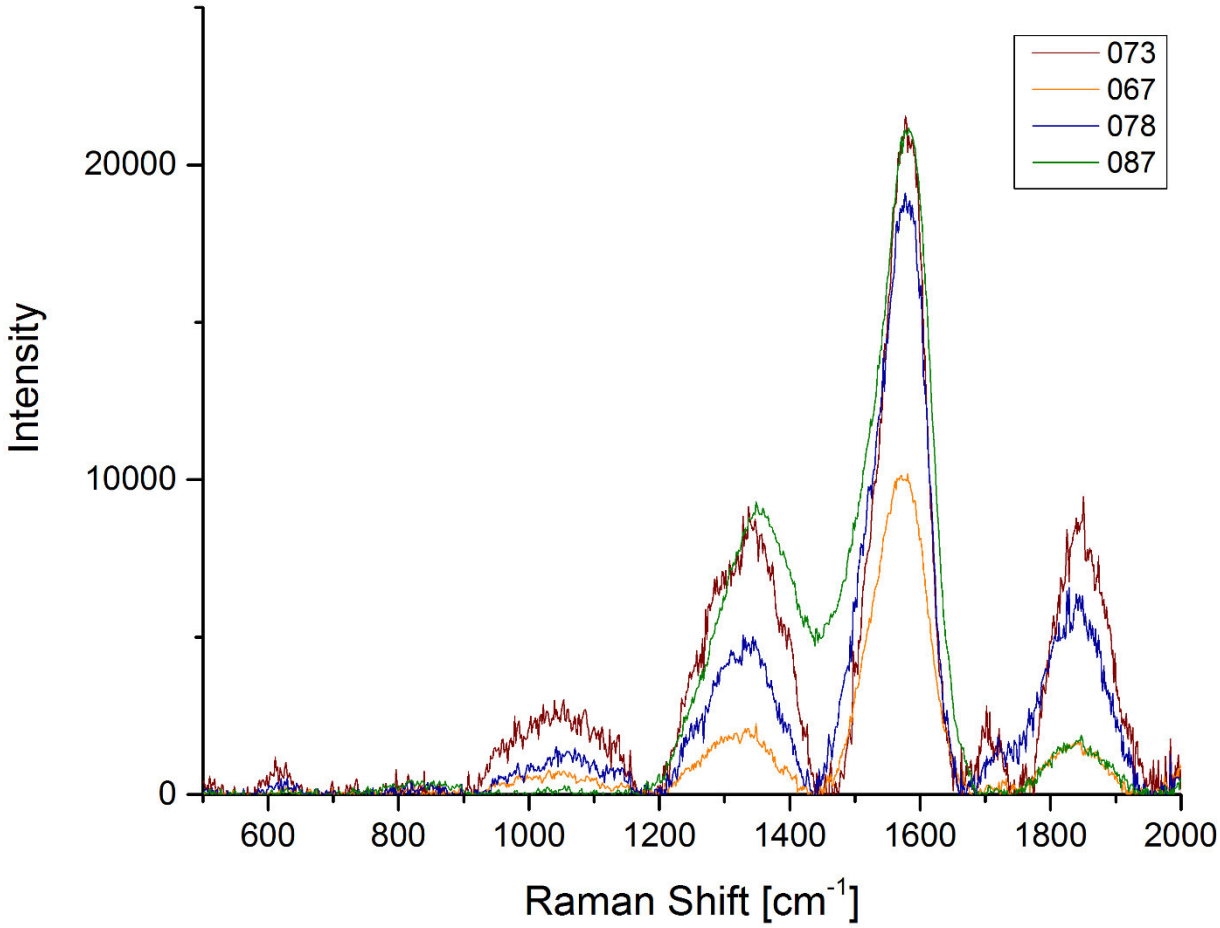

Figure 8: Raman spectra for samples 067, 073, 078 and 087. D and G peak at approximately 1350 cm^{-1} and 1570 cm^{-1} respectively.

The D peak position difference for sample 087 compared to the other ones indicates strained sp^3 hybridized bonds in this sample. The differences of intensity between the samples indicate that the concentration of present materials changes. Furthermore the different full widths of D and G peaks indicate that the amount of amorphous phases varies. Hence the samples were not coated with the same DLC films.

5.3 Surface Roughness Measurements

Table 4 shows mean values with associated standard deviation of root-mean-squared surface roughness before ($R_{q,\ pre\ DLC}$) and after ($R_{q,\ post\ DLC}$) DLC coating and the changes of root-mean-squared surface roughness (ΔR_q).

Table 4: Mean with associated standard deviation of root-mean-squared roughness values for each pair of coating process and pretreatment.

Deposition process	Blasting material	$R_{q,\ pre\ DLC}$ [nm]	$R_{q,\ post\ DLC}$ [nm]	ΔR_q [nm]
3 µm Monolayer	Fine	682.26 ± 224.65	732.72 ± 238.19	50.46 ± 41.69

Deposition process	Blasting material	$R_{q,\ pre\ DLC}$ [nm]	$R_{q,\ post\ DLC}$ [nm]	Δ R_q [nm]
3 µm Multilayer	Fine	559.14 ± 42.71	675.35 ± 171.09	116.21 ± 156.39
5 µm Multilayer	Fine	534.81 ± 53.71	620.70 ± 54.71	85.89 ± 66.28
	Coarse and Fine	1326.51 ± 149.64	1264.96 ± 202.47	-61.54 ± 75.36
	Coarse	2067.67 ± 227.82	2062.50 ± 159.65	-5.17 ± 314.35
10 µm Multilayer	Fine	725.87 ± 144.62	783.72 ± 161.38	57.85 ± 106.86
	Coarse and Fine	1195.12 ± 143.36	1244.95 ± 215.55	49.82 ± 136.87
	Coarse	1906.38 ± 180.29	1998.60 ± 212.16	92.32 ± 180.82
20 µm Multilayer	Fine	727.12 ± 134.37	1316.64 ± 139.02	589.52 ± 134.15
	Coarse and Fine	2083.69 ± 246.68	2316.46 ± 276.27	232.77 ± 305.81

There are high variations in the changes of surface roughness pre and post DLC coating. This can be seen by the standard deviations in Table 4 and in Figure 9, which illustrates the changes of R_q of fine sandblasted samples for all deposition processes. The red lines denote the median values for corresponding group of samples. Strongly varying data points are illustrated with red crosses.

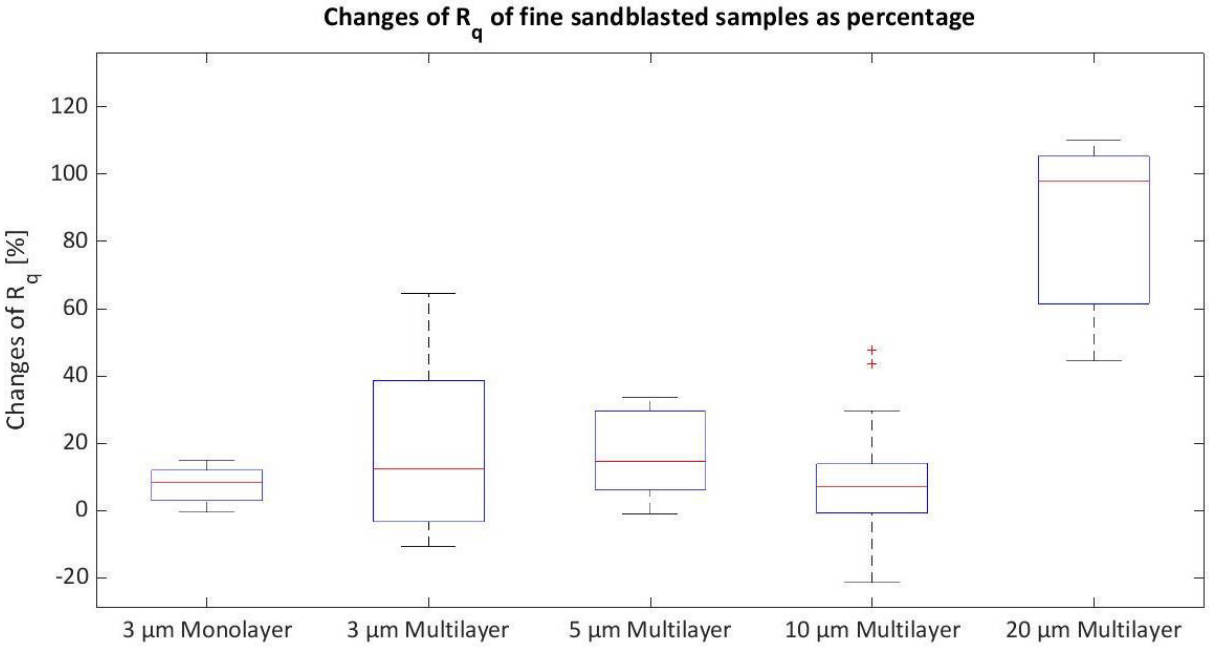

Figure 9: Box plots showing changes in R_q pre and post DLC deposition of fine sandblasted samples for all applied deposition processes.

There was no clear pattern observed in changes of surface roughness between pre and post DLC coating for none of the three pretreatment methods.

Levene's Test was used to evaluate equality of variances of surface roughness values within deposition processes. Resulting p-value (p = 0.0084) indicates unequal variances of surface roughness values within deposition processes. Therefore Kruskal-Wallis ANOVA was used to investigate if changes of surface roughness pre and post DLC depend on film thickness of DLC. The results of Kruskal-Wallis ANOVA for comparison of 3, 5, 10 and 20 µm of fine sandblasted samples are shown in Table 5.

Table 5: Kruskal-Wallis ANOVA Table for comparison of 3, 5, 10 and 20 µm of fine sandblasted samples. Thereby SS denotes the sum of squares, dF the degrees of freedom, MS the mean squares, Chi² the Chi²-statistic and p the p-value.

Type of variability	SS	dF	MS	Chi²	p
Between groups	3574.9	4	893.715	13.93	0.0075
Within groups	10285.1	50	205.703	-	-
Total	13860	54	-	-	-

The p-value indicates rejection of the null hypothesis that population means are the same. Hence there is strong evidence that at least one of the means differs significantly. Box plots show that 20 µm Multilayer is the outliner, which causes this result. Hence Kruskal-Wallis ANOVA was applied again excluding 20 µm Multilayer.

Results of Kruskal-Wallis ANOVA for comparison of 3, 5 and 10 µm of fine sandblasted samples are shown in Table 6.

Table 6: Kruskal-Wallis ANOVA Table for comparison of 3, 5and 10 µm of fine sandblasted samples. Thereby SS denotes the sum of squares, dF the degrees of freedom, MS the mean squares, Chi the Chi²-statistic and p the p-value.

Type of variability	SS	dF	MS	Chi²	p
Between groups	245.5	3	81.847	1.16	0.7637
Within groups	10167	46	221.021	-	-
Total	10421.5	49	-	-	-

The p-value indicates the acceptation of the null hypothesis that population means are the same. Hence there is no statistical significant difference between the changes of surface roughness pre and post DLC of 3, 5 and 10 µm film thickness.

5.4 Laser Markability

The visual examination showed that in all circles it was ablated enough that a mark remains, as it can be seen in Figure 5 in chapter 4.5 Laser Markability. More accurate visual inspection by microscope with 50 fold magnification revealed that in 5 of 22 laser ablated circles throughout the entire circle line DLC coating was removed and stainless steel exposed. An example is illustrated in Figure 10.

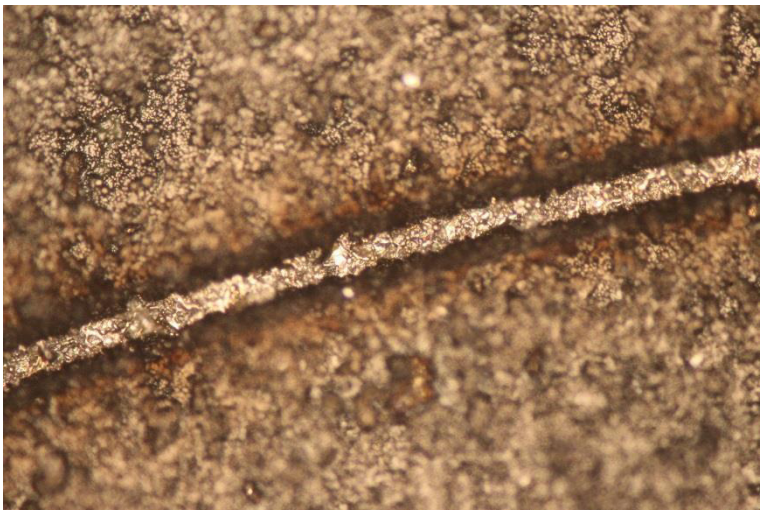

Figure 10: Example for laser ablated circle line of which the entire coating was removed and stainless steel is exposed. Picture was taken with 50 fold magnification.

Furthermore small defects of DLC coating were detected on 11 of 22 circle lines. An example is illustrated in Figure 11, the arrow indicated the defect on the circle line.

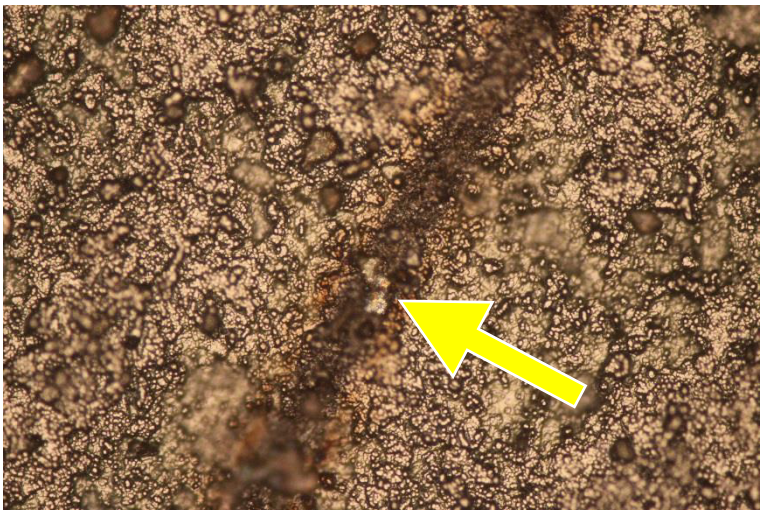

Figure 11: Example for laser ablated circle line which shows small defects. The defect, where stainless steel is exposed, is shown by an arrow. Picture was taken with 50 fold magnification.

However no defects of DLC coating after laser ablation were detected in 6 of 22 circles. An example is illustrated in Figure 12.

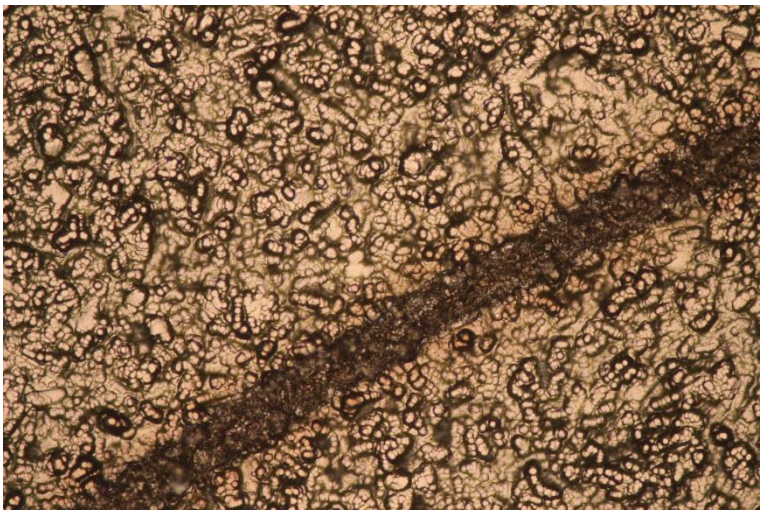

Figure 12: Example for laser ablated circle line without any defects. Picture was taken with 50 fold magnification.

Table 7 gives an overview of the results from visual inspection by microscope with 50 fold magnification of all laser ablated circle lines.

Table 7: Results of visual inspection by microscope with 50 fold magnification.

Circle	Result of visual inspection
1	Entire circle line removed.
2	Entire circle line removed.
3	Entire circle line removed.
4	Small defects detected.
5	Small defects detected.
6	**No defects detected.**
7	Entire circle line removed.
8	**No defects detected.**
9	Small defects detected.
10	Small defects detected.
11	**No defects detected.**
12	**No defects detected.**
13	Small defects detected.
14	Small defects detected.
15	Small defects detected.
16	Small defects detected.
17	**No defects detected.**
18	**No defects detected.**
19	Small defects detected.
20	Small defects detected.

Circle	Result of visual inspection
21	Entire circle line removed.
22	Small defects detected.

The settings of the laser, which were used to create defect free laser marks in circle 6, 8, 11, and 17 showed in other cases defects in DLC coating after laser ablation.

6 Discussion

6.1 Pretreatment and DLC Deposition

Pretreatment of samples by sandblasting occurred to improve adhesion of DLC coatings to stainless steel. According to Ohana et al. [37] adhesion of DLC coatings is enhanced by a rough substrate surface. Hence absence of flaking is due to increased surface roughness of sandblasted samples.

Since samples, coated by the same process in different runs, showed varying colors of DLC coating, the suspicion raised that DLC coatings with different compositions were deposited. This suspicion is supported by the results of Raman spectroscopy, which showed that the samples were not coated with the same DLC. Hence the predefined deposition processes deliver not reproducible DLC coatings. A reason for different coatings despite consistent parameters might be the PECVD system. A defect or special configurations might impair gas inlet, coupling of the generator or proper functioning of soft and hardware.

6.2 Experimental Examinations

Raman spectroscopy with inVia Qontor Raman microscope detects only D and G peak of DLC [28]. T peak might have given more information about composition of deposited DLC. However due to the wavelength of in Via Qontor Raman microscope's laser it was not possible to detect T peak [28].

Surface roughness measurements by DektakXT Stylus Profiler showed high variability of roughness values. Since DektakXT Stylus Profiler measures surface topography one-dimensional by stroking with a diamond tip [31], scratches on samples, which are due to manufacturing, can easily alter the actual roughness of a sample.
Kruskal-Wallis ANOVA of changes in surface roughness pre and post DLC for comparison of 3, 5, 10 and 20 µm DLC thickness of fine sandblasted samples showed that at least one mean of a group differs statistically significant. Since layer defects alter surface roughness measurements and mainly occur in thick coatings, which could be seen with the microscope during evaluation of laser tests, 20 µm thick DLC films have been excluded.
After exclusion Kruskal-Wallis ANOVA of changes in surface roughness pre and post DLC for comparison of 3, 5 and 10 µm DLC thickness of fine sandblasted samples showed no statistical significant difference between the groups. Thus one could say surface roughness is not dependent on thickness of DLC coating, provided that layer defects only occur to a low extent. This observation contradict the findings of Salvadori et al. [38] who showed roughness of DLC films as a function of coating thickness.

Laser markability test showed that it is possible to mark DLC with a coherent linear pattern. However settings of the laser, which were used to create defect free laser ablated circles, resulted in defect DLC coatings when applied another time. In order to maintain defect free DLC coating after laser ablation, further investigation is necessary.
Laser marked UDI code needs to be readable by a barcode [4]. Hence further investigations are necessary to evaluate if it is possible to mark a UDI code by laser ablation and if this code is readable by barcode scanner.

7 Conclusion

Results of laser markability test show that it is possible to mark DLC coating with a coherent line pattern by laser ablation. Nevertheless further investigations are necessary in order to evaluate if it is possible to mark a UDI code by laser ablation and if this code is readable by barcode scanners.

Moreover it was shown that surface roughness of DLC coatings does not hinge on thickness of the DLC coatings, provided that layer defects only occur to a low extent. Additionally it was confirmed that a rough surface enhances adhesion of DLC to stainless steel.

Notwithstanding the current configuration of the PECVD coating system cannot be used to perform reproducible coating processes and improvement measures are indispensable to guarantee reliable deposition of unvarying DLC coatings.

References

[1] R. Kramme, Medizintechnik, Springer Berlin Heidelberg, Berlin, Heidelberg, 2017.

[2] Axyn-Tec Dünnschichttechnik GmbH, Chirurgische Instrumente dauerhaft schützen: Kratzfeste und blendarme Oberflächen, Journal für Oberflächentechnik (2014) 24–25.

[3] D.K.G. de Boer, Influence of the roughness profile on the specular reflectivity of x rays and neutrons, Phys. Rev. B 49 (1994) 5817–5820. https://doi.org/10.1103/PhysRevB.49.5817.

[4] Medical Device Regulation: (EU) 2017/745, in: Amtsblatt der Europäischen Union, L117/1 - L117/175.

[5] A. Hotta, T. Hasebe, Diamond-Like Carbon Coated on Polymers for Biomedical Applications, in: S. Nazarpour (Ed.), Thin Films and Coatings in Biology, Springer Netherlands, Dordrecht, 2013, pp. 171–228.

[6] B.J. Jones, A. Mahendran, A.W. Anson, A.J. Reynolds, R. Bulpett, J. Franks, Diamond-like carbon coating of alternative metal alloys for medical and surgical applications, Diamond and Related Materials 19 (2010) 685–689. https://doi.org/10.1016/j.diamond.2010.02.012.

[7] Y. Nitta, K. Okamoto, T. Nakatani, H. Hoshi, A. Homma, E. Tatsumi, Y. Taenaka, Diamond-like carbon thin film with controlled zeta potential for medical material application, Diamond and Related Materials 17 (2008) 1972–1976. https://doi.org/10.1016/j.diamond.2008.05.004.

[8] G. Blasek, G. Bräuer, Vakuum - Plasma - Technologien: Beschichtung und Modifizierung von Oberflächen, Leuze, Bad Saulgau, 2010.

[9] P. Arunkumar, S.K. Kuanr, K.S. Babu (Eds.), Thin Film: Deposition, Growth Aspects, and Characterization, Springer International Publishing Switzerland, 2015.

[10] R. Maheswaran, R. Sivaraman, O. Mahapatra, P.C. Rao, C. Gopalakrishnan, D.J. Thiruvadigal, Surface studies of diamond-like carbon films grown by plasma-enhanced chemical vapor deposition, Surf. Interface Anal. 42 (2010) 1702–1705. https://doi.org/10.1002/sia.3371.

[11] R.D. Gould, S. Kasap, A.K. Ray, Thin Films, in: S. Kasap, P. Capper (Eds.), Springer Handbook of Electronic and Photonic Materials, Springer International Publishing, Cham, 2017, p. 1.

[12] L. Niinistö, From Precursors to Thin Films: Thermoanalytical techniques in the thin film technology, Journal of Thermal Analysis and Calorimetry 56 (1999) 7–15. https://doi.org/10.1023/A:1010154818649.

[13] K. Wasa, Thin Films as Material Engineering, J Supercond Nov Magn 28 (2015) 1665–1680. https://doi.org/10.1007/s10948-014-2949-6.

[14] L. Eckertová, Physics of thin films: Transl. by the author, 2nd ed., Plenum Press, New York, 1990.

[15] H. Frey, H.R. Khan, Handbook of Thin-Film Technology, Springer Berlin Heidelberg, Berlin, Heidelberg, 2015.

[16] Q.J. Wang, Y.-W. Chung, Encyclopedia of Tribology, Springer US, Boston, MA, 2013.

[17] J. Böhlmark, Fundamentals of high power impulse magnetron sputtering, Linköping University, Linköping, 2006.

[18] M. Braun, Magnetron Sputtering Technique, in: A.Y.C. Nee (Ed.), Handbook of Manufacturing Engineering and Technology, Springer London, London, 2015, pp. 2929–2957.

[19] A.H. Lettington, Applications of diamond-like carbon thin films, Carbon 36 (1998) 555–560. https://doi.org/10.1016/S0008-6223(98)00062-1.

[20] Verein Deutscher Ingenieure, VDI 2840 Kohlenstoffschichten: Grundlagen, Schichttypen und Eigenschaften, Beuth Verlag GmbH, Berlin, 2012.

[21] M. Łępicka, M. Grądzka-Dahlke, Surface Modification of AISI 440B Stainless Steel and its Influence on Surgical Drill Bits Performance, Archives of Metallurgy and Materials 61 (2016) 1417–1424. https://doi.org/10.1515/amm-2016-0232.

[22] R.J. Narayan, Nanostructured diamondlike carbon thin films for medical applications, Materials Science and Engineering: C 25 (2005) 405–416. https://doi.org/10.1016/j.msec.2005.01.026.
[23] B. Bhushan, Nanotribology of Ultrathin and Hard Amorphous Carbon Films, in: B. Bhushan (Ed.), Nanotribology and Nanomechanics, Springer International Publishing, Cham, 2017, pp. 593–640.
[24] T. Beatty, Everything You Need to Know about UDIs, 2013. https://www.mddionline.com/everything-you-need-know-about-udis.
[25] Naturwissenschaftliches und Medizinisches Institut, Homepage. https://www.nmi.de/de/.
[26] A.C. Ferrari, Determination of bonding in diamond-like carbon by Raman spectroscopy, Diamond and Related Materials 11 (2002) 1053–1061. https://doi.org/10.1016/S0925-9635(01)00730-0.
[27] A.C. Ferrari, J. Robertson, Resonant Raman spectroscopy of disordered, amorphous, and diamondlike carbon, Phys. Rev. B 64 (2001) 199. https://doi.org/10.1103/PhysRevB.64.075414.
[28] Renishaw pld., Handbook: inVia Qontor Raman Microscope.
[29] Deutsches Institut für Normung, DIN EN ISO 25178 Geometrische Produktspezifikation (GPS): Oberflächenbeschaffenheit: Flächenhaft, Beuth Verlag GmbH, Berlin.
[30] J. Raja, B. Muralikrishnan, S. Fu, Recent advances in separation of roughness, waviness and form, Precision Engineering 26 (2002) 222–235. https://doi.org/10.1016/S0141-6359(02)00103-4.
[31] Bruker Corporation, Handbook: DektakXT Stylus Profiler.
[32] B. Muralikrishnan, J. Raja, Gaussian Regression Filters, in: Computational Surface and Roundness Metrology, Springer London, London, 2009, pp. 67–76.
[33] E. Mooi, M. Sarstedt, I. Mooi-Reci (Eds.), Market Research, Springer Singapore, Singapore, 2018.
[34] G. Dumitru, V. Romano, H.P. Weber, S. Pimenov, T. Kononenko, M. Sentis, J. Hermann, S. Bruneau, Femtosecond laser ablation of diamond-like carbon films, Applied Surface Science 222 (2004) 226–233. https://doi.org/10.1016/j.apsusc.2003.08.031.
[35] G. Dumitru, V. Romano, H.P. Weber, S. Pimenov, T. Kononenko, J. Hermann, S. Bruneau, Y. Gerbig, M. Shupegin, Laser treatment of tribological DLC films, Diamond and Related Materials 12 (2003) 1034–1040. https://doi.org/10.1016/S0925-9635(02)00372-2.
[36] LPKF Laser & Electronics AG, Handbook: ProtoLaser U.
[37] T. Ohana, M. Suzuki, T. Nakamura, A. Tanaka, Y. Koga, Tribological properties of DLC films deposited on steel substrate with various surface roughness, Diamond and Related Materials 13 (2004) 2211–2215. https://doi.org/10.1016/j.diamond.2004.06.037.
[38] M.C. Salvadori, D.R. Martins, M. Cattani, DLC coating roughness as a function of film thickness, Surface and Coatings Technology 200 (2006) 5119–5122. https://doi.org/10.1016/j.surfcoat.2005.05.030.